



**HAL**  
open science

# Modelling a simplified device-a wind musical instrument-as an educational tool to study the behavior of a one-dimensional resonator

Catherine Potel, Michel Bruneau, Philippe Gatignol

► **To cite this version:**

Catherine Potel, Michel Bruneau, Philippe Gatignol. Modelling a simplified device-a wind musical instrument-as an educational tool to study the behavior of a one-dimensional resonator. *Journal of the Acoustical Society of America*, 2023, 154 (6), pp.3842-3850. 10.1121/10.0023959 . hal-04352877

**HAL Id: hal-04352877**

**<https://hal.science/hal-04352877v1>**


Submitted on 19 Dec 2023

**HAL** is a multi-disciplinary open access archive for the deposit and dissemination of scientific research documents, whether they are published or not. The documents may come from teaching and research institutions in France or abroad, or from public or private research centers.

L'archive ouverte pluridisciplinaire **HAL**, est destinée au dépôt et à la diffusion de documents scientifiques de niveau recherche, publiés ou non, émanant des établissements d'enseignement et de recherche français ou étrangers, des laboratoires publics ou privés.

Copyright

## Modelling a simplified device—a wind musical instrument—as an educational tool to study the behavior of a one-dimensional resonator

Catherine Potel,<sup>1,a)</sup>  Michel Bruneau,<sup>1</sup> and Philippe Gagnon<sup>2</sup>

<sup>1</sup>Laboratoire d'Acoustique de l'Université du Mans (LAUM), UMR 6613, Institut d'Acoustique - Graduate School (IA-GS), CNRS, Le Mans Université, Le Mans, 72085 Cedex 9, France

<sup>2</sup>Alliance Sorbonne Université, Université de Technologie de Compiègne, Laboratoire Roberval, FRE UTC/CNRS 2012, CS 60319, 60203 Compiègne Cedex, France

### ABSTRACT:

The aim of this paper is to show how the analytical modelling of a simplified acoustic device (herein a simplified wind musical instrument) may be a relevant educational way to study several aspects of the behavior of an idealized component [herein a one-dimensional (1-D) resonator], which is the core component of the device considered. A time-dependent source, whether sinusoidal, impulse, or representing approximate valve-effects of the reed, is coupled to the resonator in the analytical modelling. The unavoidable thermo-viscous parietal dissipation, as well as an approximate radiation effect, are accounted for. After a brief presentation of the problem, precisely posed and solved in detail analytically in an approximate manner, results in both the frequency domain and in the time domain are presented. These results include the properties of the transient behaviors (both the starting transient and the transient decay), illustrating the main features of the resonator. © 2023 Acoustical Society of America.

<https://doi.org/10.1121/10.0023959>

(Received 14 July 2023; revised 28 November 2023; accepted 29 November 2023; published online 18 December 2023)

[Editor: Preston Scot Wilson]

Pages: 3842–3850

### I. INTRODUCTION

The intent of the paper is to show, through an example, how to deepen the understanding of the behavior of an idealized acoustic component [herein a one-dimensional (1-D) resonator] by analytically modelling a simplified acoustic device, the core of which is nothing but this acoustic component (herein, a simplified wind musical instrument). In other words, we would like to answer the question of how the modelling of a simplified acoustic device may be a relevant educational way to study several aspects of the behavior of an idealized component which is the core component of the device considered. More specifically, the fundamental behavior in the frequency domain of a rigid-walled cylindrical tube of finite length, closed at one end and open at the other end (Fig. 1), considered as an idealized component excited below its cutoff frequency, is understood by students very early in their studies (Bachelor's degree). However, a more advanced device, where both a time-dependent source is coupled to the resonator and the unavoidable thermo-viscous parietal dissipation is taken into account,<sup>1–3</sup> allows the more advanced students (Master's degree) to gain a deeper understanding of the phenomena that can take place in such a device. Note that these phenomena include the properties of the transient behaviors, both the starting transient and the transient decay. Moreover, by making the transition from an academic problem to a real system (even if it

is drastically simplified), herein a simplified clarinet where the source term is given by the valve-effect of the mouth-piece<sup>4</sup> (simplified as much as possible while retaining the fundamental operating principle),<sup>5,6</sup> should challenge the student to apply conceptual understanding to a problem-solving ability and should hold its interest. Note that the subject of the paper has been presented previously, among other subjects, but in a drastically reduced version,<sup>6</sup> in order to illustrate the purpose of the paper (the training of the students through exercises).

The paper is divided into sections as follows: After this introductory Sec. I, the analytical approach (the problem and its approximate solution) is presented in Sec. II, which is divided into two subsections: the fundamental equations and hypotheses assumed are presented in Sec. II A, then the corresponding approximate analytical solution is outlined in Sec. II B. Before concluding (Sec. IV), Sec. III presents successively the fields created by three particular particle velocity sources (set at the entrance of the resonator): time periodic particle velocity source (Sec. III A), instantaneous impulse particle velocity source (Sec. III B), and valve-effect particle velocity source (Sec. III C).

### II. THE PROBLEM POSED AND ITS APPROXIMATE SOLUTION

To illustrate the objective presented in Sec. I, we present here the method used to model a simplified clarinet (as described in Ref. 5). The system considered is a dissipative cylindrical rigid-walled tube of radius  $a$  and of finite length  $L$

<sup>a)</sup>Email: catherine.potel@univ-lemans.fr

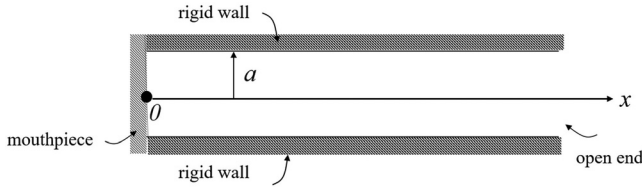


FIG. 1. Rigid-walled cylindrical tube of finite length open at one end and closed at the other end ( $x = 0$ , mouthpiece either closed or open with a quasi-static pressure higher in the oral cavity than in the mouthpiece).

(distance between the entrance of the mouthpiece and the first open hole), coupled to a particle velocity source at its entrance. This tube can be considered as closed at one end and open at the other end (Fig. 1). For such a cylindrical tube of constant radius “ $a$ ,” the assumption of plane wave propagation can be used up to its first cutoff frequency  $f_c = 1,84 c_0 / (2 \pi a)$ ,  $c_0$  being the speed of sound in the air ( $c_0 = 340 \text{ m}\cdot\text{s}^{-1}$ ). The dissipative effects in the tube are those that occur inside the thermo-viscous boundary layers. They depend on the square root of the angular frequency. Accordingly, the propagation equation in the time domain involves a half-order derivative with respect to the time, which leads to a problem that is nearly unmanageable. This is why the analytical model is initially based on the propagation equation expressed in the frequency domain. It is then simplified as much as possible while retaining the essential characteristics of the system being studied (a simplified clarinet). These characteristics include the transient behaviors (starting transient and transient decay) of the resonator and the valve-effect of the source composed of the mouthpiece and the reed. Note that the radius  $a$  of the clarinet is such that  $a = 7 \cdot 10^{-3} \text{ m}$  and that the length  $L$  is chosen such that  $L = 0.4 \text{ m}$  [which corresponds, for a B-flat clarinet, to a sounding pitch  $G_3$  sharp ( $\approx 206.9 \text{ Hz}$ )].

### A. The fundamental equations and hypotheses

Let  $\hat{\Phi}(x)$  designate the Fourier transform of the velocity potential  $\varphi(x, t)$ ,  $c_0$  the adiabatic speed of sound,  $\rho_0$  the density,  $\ell'_v$  and  $\ell'_h$  the viscous and thermal characteristic lengths of the gas,<sup>1</sup>  $\omega$  the angular frequency,  $k_0 = \omega/c_0$  the adiabatic wave number,  $\hat{V}_0(\omega)$  the Fourier transform of the velocity  $\hat{v}_0(t)$  of the source set at the entrance  $x = 0$  of the tube,  $L$  the length of the tube,  $\delta(x)$  the Dirac delta function, and  $\hat{V}_0(\omega) \delta(x)$  the volume velocity of the source (the “hats” represent variables that take complex values). Then, employing several results available in the literature<sup>4,7,8</sup> that pave the way for modeling the dissipative and reactive effects of the thermo-viscous boundary layers (Appendix), it follows that the approximate propagation equation for the velocity potential in the frequency domain (which shows a complex wave number) takes the form

$$\frac{d^2 \hat{\Phi}(x)}{dx^2} + \left(1 + \eta \frac{\exp(-i\pi/4)}{\sqrt{\omega}}\right) \frac{\omega^2}{c_0^2} \hat{\Phi}(x) = \hat{V}_0(\omega) \delta(x), \quad x \in (0, L), \quad (1)$$

where the dimensionless factor  $\eta/\sqrt{\omega}$  involves the square root of the angular frequency and the thermo-viscous

real parameter  $\eta = 2(\sqrt{c_0}/a)[\sqrt{\ell'_v} + (\gamma - 1)\sqrt{\ell'_h}]$ , both expressed in terms of the same SI unit, namely, expressed in  $\text{s}^{-1/2}$  because of the presence of a square root in each of them (for air under standard conditions  $\eta/\sqrt{2} \cong 1 \text{ s}^{-1/2}$ ). The well-posed problem can then be written as follows:

$$\left\{ \frac{d^2}{dx^2} - i\omega \varepsilon_\omega + (1 + \sigma_\omega) \frac{\omega^2}{c_0^2} \right\} \hat{\Phi}(x) = \hat{V}_0(\omega) \delta(x), \quad (2)$$

$$\frac{d\hat{P}(x)}{dx} = 0, \quad x = 0, \quad (3)$$

$$\left\{ \frac{d}{dx} + i \frac{\omega/c_0}{\hat{\zeta}(\omega)} \right\} \hat{\Phi}(x) = 0, \quad x = L, \quad (4)$$

with

$$\varepsilon_\omega = \frac{\eta\sqrt{\omega}}{\sqrt{2}c_0^2}, \quad (5a)$$

$$\sigma_\omega = \frac{\eta}{\sqrt{2}\sqrt{\omega}}, \quad (5b)$$

and where  $\hat{\zeta}(\omega)$  is a specific acoustic impedance (here, the specific radiation impedance). Note that the effect of the localized source could have been taken into account in the form of boundary condition:  $d\hat{P}(x)/dx = -i\omega \rho_0 \hat{V}_0(\omega)$  at  $x = 0$ , where  $\hat{P}(x) = -i\omega \rho_0 \hat{\Phi}(x)$  is the pressure variation in the frequency domain.

In order to match the approximations obtained here, the following comments should be noted:

- (1) the pitch range of the B-flat clarinet, from sounding pitch  $D_3$  (164.8 Hz) to  $F_6$  (1568 Hz), even to  $B_7$  flat (1865 Hz) attainable by advance players, which defines the frequency range to be considered;
- (2) the half-tone defined as the relative frequency difference  $(\Delta f/f)_{1/2} = 2^{1/12} - 1 = 0.06$ ;
- (3) the separation between successive resonances, given approximately by  $(\Delta f/f)_{1/2} \cong 0.06$ , the maximum relative width of the  $m^{\text{th}}$  resonance  $f_m$  being given by  $[\Delta f]_{-3\text{dB}}/f_m]_{\text{max}} \cong 0.03$ .

In order to simplify the model as much as possible, while conserving the essential characteristics of the resonator of the clarinet, the following approximations can be obtained:

- (1) A first approximation is that no sound is radiated at all from the instrument because the acoustic pressure amplitude in the sound wave radiated is remarkably small in comparison with the acoustic amplitude in the interior of the resonator. This approximation provides a good basis for modelling the resonator of the instrument because the energy absorption at the wall is much greater than the energy radiated from the end of the resonator. Then, the real part of the radiation impedance  $\hat{\zeta}(\omega)$ , proportional to  $(ka)^2$ , is neglected in comparison with its imaginary part  $8ka/(3\pi)$ ,<sup>1</sup> assuming that

$ka \ll 1$  ( $k = \omega/c_0$  is the wavenumber and  $a$  the radius of the resonator). This approximate expression of the imaginary part is such that the parameter  $i(\omega/c_0)/\hat{\zeta}(\omega) \cong 3\pi/(8a)$  in Eq. (4) is real and independent of the frequency, and it implies that the effective pressure node, set at the geometrical end of the tube when we assume a Dirichlet boundary condition, is displaced beyond by a distance  $8a/(3\pi)$ .

- (2) A pressure change in the mouthpiece (considered as the entrance of the resonator) modifies the rate at which air flow passes through the slit between the reed and the mouthpiece, which, in turn, changes the pressure in the mouthpiece. A second approximation is that, in this valve-effect of the vibrating reed coupled strongly with the resonator, the behavior of the reed, damped by the lower lip and coupled with the mouth cavity of the player, can be simplified as much as possible while retaining the fundamental operating principle of the coupling system (valve-effect).
- (3) The parameters  $\varepsilon_\omega$  and  $\sigma_\omega$  are smoothly varying functions of  $\omega$ : their relative variation over the relative width  $[\Delta f]_{-3\text{dB}}/f_m]_{\text{max}} \cong 0.03$  of any resonance peak (which are separated from each other) is given readily by  $\Delta\varepsilon_\omega/\varepsilon_\omega \cong \Delta\sigma_\omega/\sigma_\omega \cong 0.015$  so that they can be assumed to be constant in these intervals  $(\Delta\omega_m)_{-3\text{dB}}$ . Then, a third approximation is that these parameters depend only on the discretized eigenfrequencies of the resonator:

$$\varepsilon_\omega = \frac{\eta\sqrt{\omega}}{\sqrt{2}c_0^2} \quad \text{and} \quad \sigma_\omega = \frac{\eta}{\sqrt{2}\sqrt{\omega}}$$

are replaced by

$$\varepsilon_m = \frac{\eta\sqrt{\omega_m}}{\sqrt{2}c_0^2} \tag{6a}$$

and

$$\sigma_m = \frac{\eta}{\sqrt{2}\sqrt{\omega_m}}, \tag{6b}$$

respectively.

### B. The modal solution

The construction of the solution in terms of eigenmodes of the resonator makes use of modal wave functions  $\Psi_m$  and the modal wave number  $\tilde{k}_m$  satisfying the boundary conditions at both ends of the resonator [Eqs. (3) and (4)]. They are orthogonal because the radiation parameter  $(\omega/c_0)/\hat{\zeta}(\omega)$  is an imaginary number independent of the frequency as mentioned above.

The boundary problem takes the following form ( $\tilde{k}_m = \tilde{\omega}_m/c_0$ ):

$$\left\{ \frac{d^2}{dx^2} + \tilde{k}_m^2 \right\} \Psi_m(x) = 0, \quad x \in (0, L), \tag{7}$$

$$\frac{d}{dx} \Psi_m(x) = 0, \quad x = 0, \tag{8}$$

$$\left\{ \frac{d}{dx} + \frac{3\pi}{8a} \right\} \Psi_m(x) = 0, \quad x = L. \tag{9}$$

The well-known solutions are given by

$$\Psi_m(x) = \cos(\tilde{k}_m x), \tag{10}$$

$$\tilde{k}_m L \sin(\tilde{k}_m L) = \frac{3\pi L}{8a} \cos(\tilde{k}_m L), \tag{11}$$

leading approximately to, in assuming  $8a/(3\pi L) \ll 1$ ,

$$\tilde{k}_m \cong k_m \left( 1 - \frac{8a}{3\pi L} \right), \quad \text{with} \quad k_m = \left( m + \frac{1}{2} \right) \frac{\pi}{L}. \tag{12}$$

The orthogonality of the eigenfunctions can be verified as follows:

$$\begin{aligned} & \int_0^L \left[ \Psi_n(x) \frac{d^2}{dx^2} \Psi_m(x) - \Psi_m(x) \frac{d^2}{dx^2} \Psi_n(x) \right] dx \\ &= \left[ \Psi_n(x) \frac{d}{dx} \Psi_m(x) - \Psi_m(x) \frac{d}{dx} \Psi_n(x) \right]_0^L \\ &= (\tilde{k}_n^2 - \tilde{k}_m^2) \int_0^L \Psi_n(x) \Psi_m(x) dx. \end{aligned}$$

Owing to the boundary conditions given by Eqs. (8) and (9), this function vanishes. This implies the orthogonality of the eigenfunctions. Note that

$$\int_0^L \Psi_m^2(x) dx = \frac{L}{2} \left( 1 + \frac{8a}{3\pi L} \right).$$

The velocity potential in the Fourier domain is then expressed by the sum

$$\hat{\Phi}(x) = \sum_{m=0}^{\infty} \hat{B}_m(\omega) \Psi_m(x). \tag{13}$$

Substitution of Eqs. (13), (6a), and (6b) into the propagation Eq. (2) indicates (in assuming the orthogonality property and after some algebra) that the inverse Fourier transform  $\hat{b}_m(t)$  of the coefficients of the expansion  $\hat{B}_m(\omega)$  obey the following equation:

$$\left\{ \frac{d^2}{dt^2} + 2r_m \frac{d}{dt} + \Omega_m^2 \right\} \hat{b}_m(t) = -\frac{2}{L} c_0^2 \hat{v}_0(t), \tag{14a}$$

where

$$\Omega_m^2 = \omega_m^2 (1 - \varsigma - \sigma_m), \quad 2r_m = c_0^2 \varepsilon_m, \quad \text{with} \quad \varsigma = \frac{16a}{3\pi L}. \tag{14b}$$

Note that  $\omega_m = c_0 k_m$  is the eigen angular frequency of the tube without losses when the open end condition is the Dirichlet condition, and that  $\Omega_m$  is the angular frequency, which accounts for the effect of the thermo-viscous boundary layers and of the imaginary part of the radiation impedance.

Note also that the Fourier transform involves all values of  $\omega$ , but, when considering the functioning of the clarinet,

the lower frequency range (say the first ten modes) is the only frequency range that is involved. The general solution for  $\hat{b}_m(t)$  is given by the convolution integral of the source term and the Green's function associated with Eq. (14),<sup>1,3,9</sup> assuming that  $r_m \ll \Omega_m$ ,

$$\hat{b}_m(t) = -\frac{2}{L} \frac{c_0^2}{\Omega_m} \int_{-\infty}^{+\infty} H(t - \tau) \exp[-r_m(t - \tau)] \times \sin[\Omega_m(t - \tau)] \hat{v}_0(\tau) d\tau, \tag{15}$$

where the Heaviside function  $H(t - \tau)$  reflects the causality.

### III. THREE PARTICULAR PARTICLE VELOCITY SOURCES AT THE ENTRANCE OF THE RESONATOR

The remainder of the paper further develops this general solution considering three particular cases, depending on the velocity profile of the source: (i) a time-periodic source leading to the well-known input impedance of the resonator of the clarinet, (ii) an instantaneous impulse source applied at  $t = 0$  (Dirac delta function) highlighting the forward and backward pulses travelling inside the tube, and (iii) the valve-effect of the reed when the player chooses a lip setting, which favors the reed vibration profile sustained by the feedback from the resonator (over several periods).

#### A. Case 1: Time-periodic particle velocity source

When the source takes the form  $\hat{v}_0(t) = V_S \exp(i\omega t)$  (harmonic source), the coefficients given by Eq. (15) can be obtained directly by using Eq. (14), leading to

$$\hat{b}_m(t) = \frac{(2/L)c_0^2 V_S \exp(i\omega t)}{\omega^2 - i\omega 2r_m - \Omega_m^2}, \tag{16}$$

and the modal expansion Eq. (13), i.e., the sought solution, is thus explicitly given by

$$\hat{\phi}(x, t) = \frac{2}{L} c_0^2 V_S \exp(i\omega t) \sum_{m=0}^{\infty} \frac{\cos(\tilde{k}_m x)}{\omega^2 - i\omega 2r_m - \Omega_m^2}. \tag{17}$$

Figure 2 shows the normalized transfer function (ratio of the acoustic pressure at  $x \geq 0$  and the volume velocity at  $x = 0$ ) denoted  $z(f)/z(f)_{\max}$  at the entrance  $x = 0$  [normalized input impedance, Fig. 2(a)], at  $x = L/3$  [Fig. 2(b)] and at  $x = L = 0, 4$  m [Fig. 2(c)], where  $z(f)$  is given by

$$z(f) = \left| \omega \sum_{m=0}^{m_{\max}} \frac{\cos(\tilde{k}_m x)}{\omega^2 - i\omega 2r_m - \Omega_m^2} \right|. \tag{18}$$

Figure 2 shows typical results of the system considered, especially the odd harmonics of the resonator of the clarinet. Note that a deviation appears when the number of calculated modes is too small, that the modelling assumes that the modes are perfectly decoupled (with  $\varepsilon_\omega \cong \varepsilon_m$  and  $\sigma_\omega \cong \sigma_m$ ), and that the validity of the model is limited to  $ka \ll 1$ , namely, to  $f \ll 10^4$  Hz.

#### B. Case 2: Instantaneous impulse particle velocity source

Here, as well as in Sec. III C, the quantities  $v_0, \phi, p, b_m, \dots$  are real quantities. With instantaneous

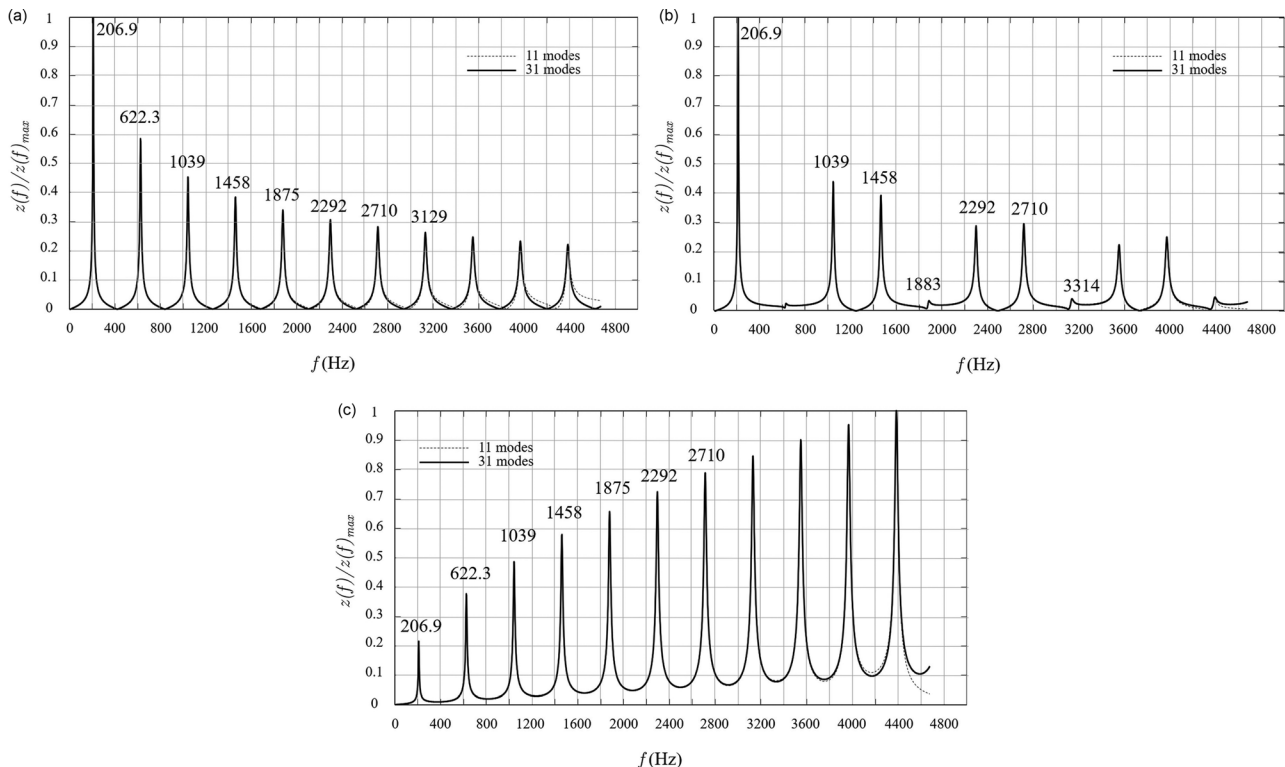


FIG. 2. Normalized transfer function  $z(f)/z(f)_{\max}$  as a function of the frequency, for the first 11 modes, with 11 modes calculated ( $m_{\max} = 10$ , dotted line) and 31 modes calculated ( $m_{\max} = 30$ , thick full line), at three abscissa: (a)  $x = 0$ , (b)  $x = L/3$ , (c)  $x = L$ .  $L = 0, 4$  m.



impulse particle velocity sources expressed as  $v_0(t) = \tilde{V}_S \delta(t)$ , Eq. (15) takes the following form ( $\tilde{V}_S$  in m):

$$b_m(t) = -\frac{2}{L} \frac{c_0^2}{\Omega_m} \tilde{V}_S \exp(-r_m t) \sin(\Omega_m t). \tag{19}$$

Thus, Eq. (17) is written as

$$\varphi(x, t) = -\frac{2}{L} c_0^2 \tilde{V}_S \sum_{m=0}^{\infty} \frac{1}{\Omega_m} \exp(-r_m t) \sin(\Omega_m t) \cos(\tilde{k}_m x). \tag{20}$$

In order to interpret this result in a simple manner, we assume the following approximation:

$$c_0 \tilde{k}_m \cong \Omega_m, \tag{21}$$

which is equivalent to making an error less than 4% on the value of the argument of the shape of the wave following the  $x$ -axis.

Then, Eq. (20) takes the following form:

$$\begin{aligned} \varphi(x, t) &= -\frac{2}{L} c_0^2 \tilde{V}_S \sum_{m=0}^{\infty} \frac{1}{\Omega_m} \exp(-r_m t) \sin(\Omega_m t) \\ &\quad \times \cos(\Omega_m x / c_0) \\ &= -\frac{2}{L} c_0^2 \tilde{V}_S \sum_{m=0}^{\infty} \frac{1}{2\Omega_m} \exp(-r_m t) \\ &\quad \times \left\{ \sin \left[ \Omega_m \left( t - \frac{x}{c_0} \right) \right] + \sin \left[ \Omega_m \left( t + \frac{x}{c_0} \right) \right] \right\}. \end{aligned} \tag{22}$$

In order to provide a basic interpretation of this result, we neglect the dissipation phenomena:  $\exp(-r_m t) \approx 1$ ; one can say in practice that the player acts on the reed of the clarinet in such a way that, at each period, the attenuation is compensated. We also neglect the end correction of the resonator:

$$\Omega_m \cong \omega_m = \left( m + \frac{1}{2} \right) \pi \frac{c_0}{L}. \tag{23}$$

Thus, the velocity potential [Eq. (22)] becomes

$$\begin{aligned} \varphi(x, t) &= -\tilde{V}_S c_0 \sum_{m=0}^{\infty} \frac{2/\pi}{2m+1} \\ &\quad \times \left\{ \sin \left[ (2m+1) \frac{\pi c_0}{2L} \left( t - \frac{x}{c_0} \right) \right] \right. \\ &\quad \left. + \sin \left[ (2m+1) \frac{\pi c_0}{2L} \left( t + \frac{x}{c_0} \right) \right] \right\}. \end{aligned} \tag{24}$$

Taking into account that the function

$$f(u) = \sum_{m=0}^{\infty} \frac{2/\pi}{2m+1} \sin(2m+1)u \tag{25}$$

is the Fourier series (modulo  $2\pi$ ) of

$$f(u) = \begin{cases} -1/2 & \text{if } -\pi < u < 0, \\ 1/2 & \text{if } 0 < u < \pi, \end{cases} \tag{26}$$

namely, of

$$f(u) = \frac{1}{2} H(u) + \sum_{n=1}^{\infty} (-1)^n H(u - n\pi), \tag{27}$$

represented in Fig. 3 (where  $H$  is the Heaviside function), the velocity potential [Eq. (24)] is readily given by

$$\begin{aligned} -\frac{\varphi(x, t)}{\tilde{V}_S c_0} &= \frac{1}{2} H \left[ \frac{\pi c_0}{2L} \left( t - \frac{x}{c_0} \right) \right] \\ &\quad + \sum_{n=1}^{\infty} (-1)^n H \left[ \frac{\pi c_0}{2L} \left( t - \frac{x}{c_0} - n \frac{2L}{c_0} \right) \right] \\ &\quad + \frac{1}{2} H \left[ \frac{\pi c_0}{2L} \left( t + \frac{x}{c_0} \right) \right] + \sum_{n=1}^{\infty} (-1)^n \\ &\quad \times H \left[ \frac{\pi c_0}{2L} \left( t + \frac{x}{c_0} - n \frac{2L}{c_0} \right) \right]. \end{aligned} \tag{28}$$

Then, the acoustic pressure  $p = -\rho_0 \partial \varphi / \partial t$  can be written as

$$\begin{aligned} \frac{p(x, t)}{\rho_0 c_0^2 \pi \tilde{V}_S / (2L)} &= \frac{1}{2} \delta \left[ \frac{\pi c_0}{2L} \left( t - \frac{x}{c_0} \right) \right] \\ &\quad + \sum_{n=1}^{\infty} (-1)^n \delta \left[ \frac{\pi c_0}{2L} \left( t - \frac{x}{c_0} - n \frac{2L}{c_0} \right) \right] \\ &\quad + \frac{1}{2} \delta \left[ \frac{\pi c_0}{2L} \left( t + \frac{x}{c_0} \right) \right] + \sum_{n=1}^{\infty} (-1)^n \\ &\quad \times \delta \left[ \frac{\pi c_0}{2L} \left( t + \frac{x}{c_0} - n \frac{2L}{c_0} \right) \right]. \end{aligned} \tag{29}$$

Figure 4 shows the forward and backward propagation of the impulse (created at the origin  $t = 0$ ) represented by this Eq. (29). The main feature is that the sign of the impulse changes when reflecting at the open end of the tube. Thus, the period of the signal corresponds to two round trips of the impulse, which is typical of the clarinet.

### C. Case 3: Valve-effect particle velocity source

When considering this last “realistic” situation in the frame of the simplified model mentioned above, the shape of the opening of the mouthpiece is rectangular (source term). The reed closes the mouthpiece only during the half-period during which the pressure at the entrance of the

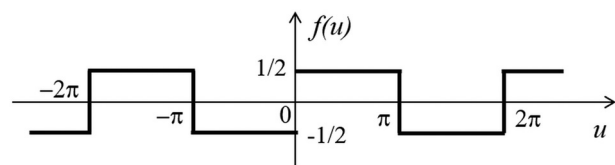


FIG. 3. Function  $f$  given by Eqs. (25), (26), or (27).

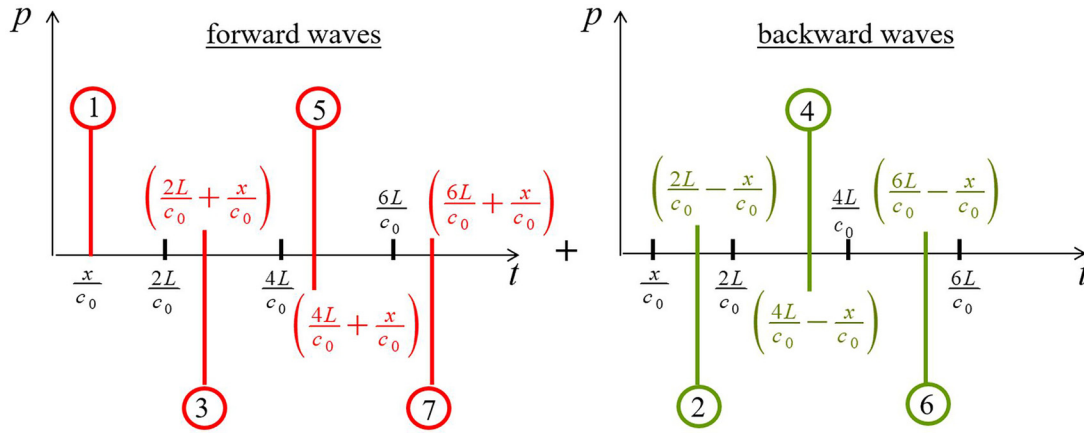


FIG. 4. (Color online) Normalized acoustic pressure as a function of time. The forward positive impulse starts at  $x = 0$  at time  $t = 0$ . It reaches the coordinate  $x$  at time  $x/c_0$  (label 1), then it is reflected at time  $L/c_0$  so that the backward negative impulse reaches the coordinate  $x$  at time  $(2L/c_0 - x/c_0)$  (label 2). Next, it is reflected at  $x = 0$  staying negative, and so on.

resonator is lower than that of the oral cavity, or in other words, it is “open” during the other half-period when the pressure at the entrance of the resonator is greater than that of the pressure in the oral cavity (everything being managed more specifically by the stiffness of the reed and by the pressure of the lips). Then, the source function  $v_0(\tau)$  takes the form of  $\ell_{\max}$  rectangular functions labelled  $\ell \in (0, \ell_{\max} - 1)$ , each one of duration  $T_0 = 2L/c_0$  (half-period of the signal) and separated from each other by the same duration  $T_0 = 2L/c_0$  (hence, the period of the signal is  $2T_0$ ):

$$v_0(\tau) = V_S \sum_{\ell=0}^{\ell_{\max}-1} \{H[\tau - 2\ell T_0] - H[\tau - (2\ell + 1)T_0]\}. \quad (30)$$

It follows directly from Eq. (15), by substituting for  $v_0$  its expression given by Eq. (30), that the pressure variation  $p = -\rho_0 \partial\varphi/\partial t$  takes the following form:

$$p(x, t) = 2 \frac{V_S}{L} \rho_0 c_0^2 \sum_{m=0}^{\infty} \frac{1}{\Omega_m} \cos\left(\frac{\Omega_m}{c_0} x\right) \times \sum_{\ell=0}^{\ell_{\max}-1} \{H[t - 2\ell T_0] \exp[-r_m(t - 2\ell T_0)] \times \sin[\Omega_m(t - 2\ell T_0)] - H[t - 2(\ell + 1)T_0] \times \exp(-r_m[t - (2\ell + 1)T_0]) \times \sin[\Omega_m(t - (2\ell + 1)T_0)]\}, \quad (31)$$

where Eq. (13) of the solution has been used.

The time dependence of the normalized pressure variation is represented by rectangular functions as shown in Fig. 5 {length of the tube 0.40 m, 51 eigen modes,  $x = 0$ , source consisting of six rectangular functions [Fig. 5(a)]}, which is characteristic of the clarinet behavior. The starting transient of the signal is shown in the next two figures, respectively, without [Fig. 5(b)] and with [Fig. 5(c)] thermo-viscous dissipation (the time range is 0–50 ms). Figure 5(d) emphasizes both the starting transient and the signal dying out in time when the source is shut off (the time range is

0–400 ms), and Fig. 5(e) shows the Fourier transform of the signal (frequency spectrum). Note that the Gibbs effect disappears when the dissipation effects are taken into account, as expected [see Eqs. (6), (14b), and (15)].

#### IV. CONCLUSION

To conclude, the core of the paper involves the analytic model of a 1-D acoustic resonator, namely, the eigenvalues and the orthogonal eigenfunctions of a waveguide closed at one end and open at the other end, providing the behavior of the idealized resonator of the simplified clarinet. In this first approach, the effect of the opening on the internal field in the tube is accounted for in assuming a pressure node just outside the end, which is due to the small imaginary part of the output impedance. The internal energy losses due to sound radiation, given by the real part of this impedance, have been assumed to be negligible because they are much smaller than the losses due to the thermo-viscous boundary layers inside the rigid-walled tube. In a second step, the model of the acoustic resonator accounts for these thermo-viscous losses, described as stepwise functions of the frequency, i.e., assumed to be almost constant in the immediate vicinity of each resonance of the tube. This approximation allows us to correctly interpret transient phenomena (transient decays). Finally, Sec. III furthers the solution of the problem in three particular cases, depending on the velocity profile of the source, including an approximate valve-effect of the reed in the third one. Overall, the paper has shown a method to study an idealized component step-by-step through the modelling of a simplified real device, to challenge the student to apply conceptual understanding to a problem-solving ability and for holding his/her interest.

To sum up, the model starts from a “well-posed” problem (propagation equation and boundary conditions) in the presence of a source in the frequency domain to avoid the fractional derivative that would appear in the time domain. In this regard, this method departs from the usual modelling found in the literature; specifically, it does not use a

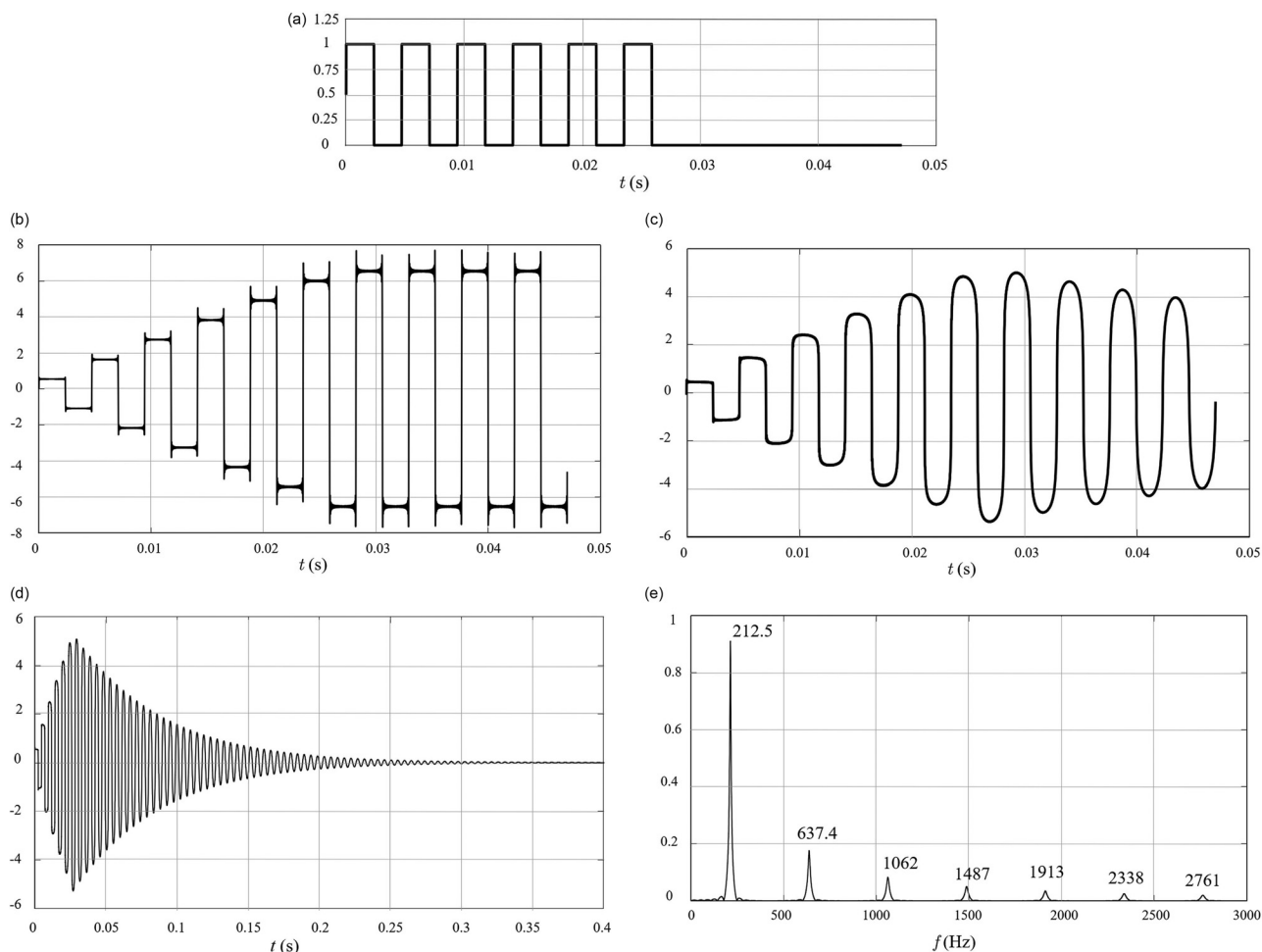


FIG. 5. Normalized acoustic pressure as a function of the time at  $x = 0$ ; (a) source: six rectangular functions of half a period each (separated from each other by a half-period), (b) without attenuation, (c) with attenuation (the time range is 0–50 ms), (d) with attenuation (the time range is 0–400 ms), (e) modulus of the Fourier transform of this field of pressure.  $L = 0, 4$  m;  $T_0 = 0,0024$  s.

transmission line model to calculate the tube impedance. In addition, three particle velocity profiles have been considered and their effects have been treated in the frequency and in the time domains. All of this should be illustrative and of interest to students at Master’s level in acoustics.

## AUTHOR DECLARATIONS

### Conflict of Interest

The authors have no conflicts to disclose.

### DATA AVAILABILITY

The data that support the findings of this study are available from the corresponding author upon reasonable request.

## APPENDIX: THE PROPAGATION EQUATION FOR THE VELOCITY POTENTIAL IN THE FREQUENCY DOMAIN

This appendix aims to demonstrate Eq. (1) outside the sources, which includes the two principal dissipative processes, namely, the effects of viscosity and thermal diffusions that take place near the tube wall. To do this, we use the three standard fundamental laws of thermo-mechanics,

i.e., the second Newton’s law, the conservation of mass equation, and the Fourier’s law of heat conduction.

### A. The first equation: Newton’s second law

The first equation considered gives the fluid acceleration in terms of the forces acting; it must include the frictional drag suffered by the fluid as it moves. This viscous force  $F$  acting on the region between the interfaces  $r$  and  $r + dr$ , of length  $dx$ , results from the shear stresses at these interfaces  $\mu 2\pi r dx \partial \hat{V}_x(r, x) / \partial r$  and  $\mu 2\pi (r + dr) dx \partial \hat{V}_x(r + dr, x) / \partial r$ , respectively, where  $r$  is the radial coordinate,  $x$  is the axial coordinate,  $\hat{V}_x$  is the particle velocity along the  $x$  axis, and where the proportionality factor  $\mu$  is the dynamic viscosity. The resultant force  $F$  then takes the following form:

$$\begin{aligned}
 F &= \mu 2\pi dx \left[ (r + dr) \frac{\partial}{\partial r} \hat{V}_x(r + dr, x) - r \frac{\partial}{\partial r} \hat{V}_x(r, x) \right] \\
 &= \mu 2\pi dx \frac{\partial}{\partial r} \left( r \frac{\partial}{\partial r} \hat{V}_x(r, x) \right) dr. \tag{A1}
 \end{aligned}$$

Applying Newton’s second law to the fluid element considered and dividing all terms by the volume  $2\pi r dx$ ,



leads to the Poiseuille’s equation relating fluid acceleration, pressure gradient, and shear viscosity force  $F$ :

$$i\omega\rho_0\hat{V}_x(r,x) = -\frac{d\hat{P}(x)}{dx} + \mu\frac{1}{r}\frac{\partial}{\partial r}\left(r\frac{\partial}{\partial r}\hat{V}_x(r,x)\right). \quad (\text{A2})$$

This equation assumes that the pressure variation is uniform over the section of the tube, that the acoustic perturbation is a quasi-plane wave, and that the effect of the bulk viscosity is negligible. The question of why these approximations are valid cannot be answered until one investigates further the viscosity effects and the thermal effects in the tube (it is beyond the scope of this Appendix).

This equation can be rewritten as follows:

$$\frac{1}{r}\frac{\partial}{\partial r}\left(r\frac{\partial}{\partial r}\hat{V}_x(r,x)\right) + k_v^2\hat{V}_x(r,x) = \frac{1}{\mu}\frac{d\hat{P}(x)}{dx} \quad (\text{A3})$$

with

$$k_v^2 = -i\omega\rho_0/\mu = -ik_0\rho_0c_0/\mu. \quad (\text{A4})$$

Its general solution is given by

$$\hat{V}_x(r,x) = \frac{-1}{i\omega\rho_0}\frac{d\hat{P}(x)}{dx} + AJ_0(k_v r) + BN_0(k_v r), \quad (\text{A5})$$

where  $J_0(k_v r)$  and  $N_0(k_v r)$  are the zero-order cylindrical Bessel function and modified Bessel function, respectively. This solution satisfies two boundary conditions, i.e., the solution remains finite at  $r = 0$  and vanishes at the wall  $r = a$ , leading readily to

$$\hat{V}_x(r,x) = \frac{-1}{i\omega\rho_0}\frac{d\hat{P}(x)}{dx}\left[1 - \frac{J_0(k_v r)}{J_0(k_v a)}\right]. \quad (\text{A6})$$

The volume velocity is given by

$$\hat{W}(x) = \int_0^a \hat{V}_x(r,x)2\pi r dr = \frac{-\pi a^2}{i\omega\rho_0}\frac{d\hat{P}(x)}{dx}\left(1 - \frac{2}{k_v a}\frac{J_1(k_v a)}{J_0(k_v a)}\right), \quad (\text{A7})$$

where  $J_1(k_v r)$  is the one-order cylindrical Bessel function.

Then, the first sought 1-D equation can be written as

$$\frac{d\hat{P}(x)}{dx} + \frac{i\omega\rho_0}{\pi a^2}\left(1 - \frac{2}{k_v a}\frac{J_1(k_v a)}{J_0(k_v a)}\right)^{-1}\hat{W}(x) = 0. \quad (\text{A8})$$

This equation reflects a radial (centripetal) diffusion movement because, compared with the acoustic wavenumber  $k_0 = \omega/c_0$ , the modulus of the viscous wavenumber  $k_v$  is very large, with equal real and imaginary parts (low diffusion speed and high attenuation). This diffusion movement originates at the boundary  $r = a$  and penetrates the fluid. Its amplitude decreases by a factor “ $e = 2.7$ ” over a short distance from the wall  $\delta_v = \sqrt{2}/|k_v| = \sqrt{2\mu/(\rho_0\omega)}$  called the “viscous boundary layer thickness,” which is much smaller than the radius of the clarinet tube.

## B. The second equation: Conservation of mass equation

The second equation is the conservation of mass equation that we need in order to remove the volume velocity  $\hat{W}(x)$  from Eq. (A8). It is written as follows ( $\varphi$  is the azimuthal coordinate):

$$i\omega\hat{\rho}' + \rho_0\left(\frac{1}{r}\frac{\partial}{\partial r}(r\hat{V}_r) + \frac{1}{r}\frac{\partial}{\partial\varphi}\hat{V}_\varphi + \frac{\partial}{\partial x}\hat{V}_x\right) = 0, \quad (\text{A9})$$

where  $\hat{\rho}'(r,x)$  is the density variation expressed below with the two independent variables  $\hat{P}(x)$  and  $\hat{\tau}(r,x)$  by the thermodynamic state law of the fluid  $\hat{\rho}'(r,x) = \gamma/c_0^2[\hat{P}(x) - \tilde{\beta}\hat{\tau}(r,x)]$ ,  $\tilde{\beta} = (\partial P/\partial T)_V$  being the increase in pressure per unit increase in temperature at constant density,  $\gamma$  being the specific heat ratio, and  $\hat{\tau}(r,x)$  being the temperature variation. After integration with respect to the variable  $r$  over the interval  $(0, a)$  and accounting for the following results:

$$\int_0^a \frac{1}{r}\frac{\partial}{\partial r}(r\hat{V}_r)r dr = a\hat{V}_r(a) = 0$$

and

$$\int_0^{2\pi} \frac{\partial}{\partial\varphi}\hat{V}_\varphi d\varphi = \hat{V}_\varphi(2\pi) - \hat{V}_\varphi(0) = 0, \quad (\text{A10})$$

Eq. (A9) takes the following form:

$$\frac{d\hat{W}}{dx} = -\pi a^2 \frac{i\omega\gamma}{\rho_0 c_0^2} [\hat{P}(x) - \tilde{\beta}\bar{\tau}(x)], \quad (\text{A11})$$

with  $\bar{\tau}(x) = \int_0^a \hat{\tau}(r,x)2\pi r dr$ .

Invoking Eq. (A11) and the derivative with respect to  $x$  of Eq. (A8), the pressure variation is governed by the 1-D equation

$$\frac{d^2\hat{P}(x)}{dx^2} + \gamma\left(\frac{\omega}{c_0}\right)^2\left(1 - \frac{2}{k_v a}\frac{J_1(k_v a)}{J_0(k_v a)}\right)^{-1}[\hat{P}(x) - \tilde{\beta}\bar{\tau}(x)] = 0. \quad (\text{A12})$$

## C. The third equation: Fourier’s law of heat conduction

The third and last equation provides the relationship between  $\hat{P}(x)$  and  $\bar{\tau}(x)$  that we need now. Near the wall  $r = a$ , the temperature variation  $\hat{\tau}(r,x)$  vanishes because the thermal conductivity and heat capacity of the wall are much greater than those of the fluid. So, near the wall, the acoustic movement is (almost) isothermal, whereas in the bulk of the fluid, it is (almost) adiabatic. A rate of heat flow takes place near the wall. This rate of heat flow is governed by the Fourier’s law of heat conduction:

$$i\omega\rho_0 T_0 \hat{\delta}(r,x) \cong \lambda_h \frac{1}{r}\frac{\partial}{\partial r}\left(r\frac{\partial}{\partial r}\right)\hat{\tau}(r,x), \quad (\text{A13})$$

where  $\hat{s}(r, x) = (C_P/T_0)(\hat{\tau}(r, x) - (\gamma - 1)/(\gamma\hat{\beta})\hat{P}(x))$  is the entropy variation,  $\lambda_h$  is the thermal conductivity, and  $C_P$  is the heat coefficient at constant pressure per unit of mass. We rewrite Eq. (A13) in the form

$$\frac{1}{r} \frac{\partial}{\partial r} \left( r \frac{\partial}{\partial r} \hat{\tau}(r, x) \right) + k_h^2 \hat{\tau}(r, x) = \frac{\gamma - 1}{\gamma\hat{\beta}} k_h^2 \hat{P}(x),$$

with  $k_h^2 = -i\omega\rho_0 C_P/\lambda_h = -ik_0\rho_0 c_0 C_P/\lambda_h$ , and we assume that the solution  $\hat{\tau}(r, x)$  satisfies two boundary conditions, i.e., the solution remains finite at  $r = 0$  and vanishes at the wall  $r = a$ . Then, after manipulations of the type employed earlier for the same mathematical problem [from Eqs. (A3)–(A7)], it follows that

$$\hat{\tau}(x) = \frac{\gamma - 1}{\gamma\hat{\beta}} \left( 1 - \frac{2 J_1(k_h a)}{k_h a J_0(k_h a)} \right) \hat{P}(x). \tag{A14}$$

The couple of Eqs. (A12) and (A14) lead readily to

$$\left( \frac{d^2}{dx^2} + \chi^2 \right) \hat{P}(x) = 0, \tag{A15}$$

where

$$\chi^2 = k_0^2 \left( 1 + (\gamma - 1) \frac{2 J_1(k_h a)}{k_h a J_0(k_h a)} \right) \left( 1 - \frac{2 J_1(k_v a)}{k_v a J_0(k_v a)} \right)^{-1}. \tag{A16}$$

It is justified retaining only the first order in the small terms which involve the asymptotic behavior of the Bessel functions, yielding

$$\chi^2 \cong k_0^2 \left( 1 + \frac{2 J_1(k_v a)}{k_v a J_0(k_v a)} + (\gamma - 1) \frac{2 J_1(k_h a)}{k_h a J_0(k_h a)} \right), \tag{A17}$$

and even

$$\chi^2 \cong k_0^2 \left( 1 + \frac{1 - i2}{\sqrt{2}} \frac{c_0}{a} \sqrt{\frac{\mu}{\rho_0 c_0}} (\ell'_v + (\gamma - 1)\ell_h) \right), \tag{A18}$$

where the characteristic lengths  $\ell'_v$  and  $\ell_h$ , defined as

$$\ell'_v = \sqrt{\frac{\mu}{\rho_0 c_0}} \quad \text{and} \quad \ell_h = \sqrt{\frac{\lambda_h}{\rho_0 c_0 C_P}}, \tag{A19}$$

are small quantities (of an order of  $10^{-8}$  m in air).

The couple of Eqs. (A15) and (A18) are none other than the Eq. (1) sought (outside the sources).

<sup>1</sup>P. M. Morse and K. U. Ingard, *Theoretical Acoustics* (McGraw-Hill, New York, 1968).  
<sup>2</sup>A. D. Pierce, *Acoustics: An Introduction to Its Physical Principles and Applications* (McGraw-Hill, New York, 1981).  
<sup>3</sup>M. Bruneau, *Manuel D'acoustique Fondamentale (Fundamentals of Acoustics)* (Hermès, Paris, 1998) (ISTE, London, 2006).  
<sup>4</sup>A. Chaigne and J. Kergomard, *Acoustics of Musical Instruments* (French ed., Belin, Paris, 2013) (Springer-Verlag, New York, 2016).  
<sup>5</sup>M. Bruneau, P. Gatignol, P. Lancelleur, and C. Potel, "Exercices d'acoustique - Corrigés détaillés. Rappels de cours" ("Exercises of acoustics - Detailed solutions. Course reminder"), in *Problèmes avancés (Advanced Exercises)* (Cépaduès, Toulouse-France, 2021), Vol. 3, pp. 246–263.  
<sup>6</sup>C. Potel, M. Bruneau, P. Gatignol, P. Lancelleur, and C. Potel, "Raising students' interest and deepening their training in acoustics through dedicated exercises," *J. Acoust. Soc. Am.* **151**(2), 1093–1103 (2022).  
<sup>7</sup>M. Campbell, J. Gilbert, and A. Myers, *The Science of Brass Instruments* (ASA Press, Springer, 2021).  
<sup>8</sup>A. Thibault and J. Chabassier, "Dissipative time-domain one-dimensional model for viscothermal acoustic propagation in wind instruments," *J. Acoust. Soc. Am.* **150**, 1165–1175 (2021).  
<sup>9</sup>S. I. Hayek, *Advanced Mathematical Methods in Science and Engineering*, 2nd ed. (CRC Press, London, 2010), Chap. 8, Sec. 8.7.